Eur. Phys. J. Special Topics **229**, 3205–3220 (2020)

https://doi.org/10.1140/epjst/e2020-000023-4

THE EUROPEAN PHYSICAL JOURNAL SPECIAL TOPICS

Review

Evading Z' boson mass limits in $U(1)'$ supersymmetric models

Mariana Frank[a]

Department of Physics, Concordia University, Montreal, Quebec H4B 1R6, Canada

Received 11 February 2020 / Accepted 30 September 2020
Published online 14 December 2020

Abstract. Supersymmetric models augmented by $U(1)'$ gauge symmetries resolve some of the outstanding problems in MSSM, such as the μ problem. Unfortunately collider phenomenology in such models is hindered by the stringent limits from the ATLAS and CMS collaborations on the Z' boson mass. We explore possibilities of lowering the mass in either leptophobic models, by employing kinetic mixing, or in models with non-universal $U(1)'$ charges, where the Z' boson does not couple either to the first two generation quarks, thus lowering its production cross-section, or to the first two generation leptons, thus lowering its di-lepton branching ratio. We verify consistency of these models with dark matter bounds and indicate the most promising signals at the collider.

1 Introduction

While the standard model (SM) of particle physics is one of the most successful theories, predicting a large number of subatomic processes based on a few fundamental parameters and basic symmetries, some outstanding issues still remain. Among these, dark matter and neutrino masses are perhaps the best experimental evidence of phenomena not predicted by the SM. Supersymmetry, in its simple form (the minimal supersymmetric standard model–MSSM), provides an answer to the former but not to the latter. Introducing a right-handed neutrino (and its scalar partner), thus enlarging the particle content of MSSM, and relying on the seesaw mechanism, would solve both problems.

But what about true unification of strong and electroweak forces? That is, instead of having the SM symmetry based on $SU(3)_c \otimes SU(2)_L \otimes U(1)_Y$, there would be a single symmetry group at a high energy scale, broken down at some lower scale to the SM (or MSSM) symmetry. It turns out that, when we try to construct a group which contains the SM as its subgroup, it is more difficult to reduce the rank of the extended group containing the SM than it is to break its non-Abelian gauge groups [1]. Extended groups, referred to as grand unified theories (GUT), have to have rank higher than 4, with $SO(10)$ and E_6 being the most popular choices [2]. Breaking these groups always involves (at least) one additional $U(1)'$ gauge group.

[a] e-mail: mariana.frank@concordia.ca

$U(1)'$ groups involve an additional neutral gauge boson associated with the group, and an additional singlet Higgs boson S to break the symmetry to that of SM/MSSM.

Introducing an additional $U(1)'$ resolves a long standing problem in MSSM, the so-called μ problem [3]. The μ is the off-diagonal Higgs/higgsino mass, which in principle can be arbitrarily large, but phenomenologically must be of the same order of magnitude as the soft-supersymmetry breaking terms. In $U(1)'$ models, this problem is elegantly solved by generating the μ parameter dynamically, through the vacuum expectation value (VEV) of the singlet $\langle S \rangle$. This VEV triggers breaking of $U(1)'$, at a scale expected to be of the same order of magnitude as the supersymmetry breaking scale. In addition, the new neutral gauge boson associated with $U(1)'$, assumed to mix minimally with the SM gauge boson Z, acquires a mass $m_{Z'}^2 \sim {Q'_S}^2 \langle S \rangle^2$, where Q'_S denotes the charge under $U(1)'$. Thus, the Z' mass is also related to this scale.

Of course, the existence of an additional neutral gauge boson has immediately attracted the attention of experimental groups, as a clearly promising evidence of physics beyond the SM. However, only disappointment followed detailed searches, as indeed any other searches for new physics. LHC collaborations have explored various signal regions for any possible hint of a Z'. The most stringent constraint up to date is derived from data accumulated at $\sqrt{s} = 13$ TeV with 139 fb^{-1} integrated luminosity [4] where high-mass dilepton resonance searches exclude Z' mass ($m_{Z'}$) up to 4.5 TeV. Searches for heavy particles decaying into top-quark pairs yield an exclusion limit on $m_{Z'}$ ranging from 3.1 TeV to 3.6 TeV at $\sqrt{s} = 13$ TeV with 36.1 fb^{-1} integrated luminosity [5], while dijet resonance search limits on $m_{Z'}$ are slightly weaker, $m_{Z'} > 2.7$ TeV at $\sqrt{s} = 13$ TeV with 36 fb^{-1} integrated luminosity [6]. Thus it is evident that the most stringent constraint on $m_{Z'}$ is derived from its leptonic decay modes. Z' mass also plays a role in fine-tuning: a high scale Z' implies a high scale $U(1)'$ physics, and an unnaturally high μ parameter, as $\mu \sim \langle S \rangle$.

In addition, Z' has been long touted as a portal for dark matter interactions [7,8], property that a high mass Z' will render ineffective. Fortunately, there are ways to evade the mass constraints: one would be to make Z' decay into di-leptons zero (leptophobic Z'), the other is to suppress Z' production (quarkophobic Z'). Reviewing these possibilities is the aim of the present article. As we shall see in the next sections, leptophobia can be achieved in two ways: universal (that is Z' does not decay into any leptons [9–12]), or non-universal (that is Z' does not decay into electrons and muons only). The $Z' \to \tau\tau$ decay can still occur in this case since the τ can decay both leptonically and hadronically. A combined search of both leptonically and hadronically decaying τ-pairs exclude $m_{Z'}$ up to 2.42 TeV at $\sqrt{s} = 13$ TeV with 36 fb^{-1} integrated luminosity [13], thus a much weaker limit.

Quarkophobia, as we shall see, can only occur if the $U(1)'$ couples non-universally to quarks: we then forbid coupling to the first two generations of quarks, while allowing coupling to top and bottom quarks. This significantly suppresses the production cross-section, alleviating the serious restrictions on Z' mass.

We proceed as follows. First, we review $U(1)'$ models, emerging from the breaking of E_6 supersymmetric GUT (while breaking $SO(10)$ in an intermediate step), in Section 2. We are particularly interested in the anomaly cancellation conditions and their implication on the $U(1)'$ charges. We then describe how to make the model leptophobic, either with universal, Section 3, or non-universal charges, Section 4.1; and how to make the non-universal $U(1)'$ model quarkophobic, in Section 4.2. We study the implications of the three scenarios and, when relevant, how to test them at the colliders. We conclude and summarize our findings in Section 5.

Table 1. Mixing angle θ_{E_6} for popular $U(1)'$ models. The value of θ_{E_6} is taken in the $[-\pi, \pi]$ range.

Model	$U(1)'_\chi$	$U(1)'_\psi$	$U(1)'_\eta$	$U(1)'_S$	$U(1)'_I$	$U(1)'_N$
θ_{E_6}	-0.5π	0	-0.79π	-0.37π	0.71π	-0.08π

2 $U(1)'$ models

We first review the theoretical framework of $U(1)'$ extended MSSM (referred to as $U(1)'$ models, for short), extensively discussed in [1,14]. The new additional states are, one extra neutral gauge boson Z', an additional singlet S, and their fermionic partners. There are several possibilities for specific $U(1)'$ symmetries. The most commonly studied $U(1)'$ extensions arise from linear combinations of the subgroups emerging from the breaking of E_6 GUTs into the SM

$$E_6 \longrightarrow SO(10) \otimes U(1)'_\psi \longrightarrow SU(5) \otimes U(1)'_\psi \otimes U(1)'_\chi. \tag{1}$$

The charges $Q'(\phi, \theta_{E_6}) = Q'_\psi(\phi) \cos\theta_{E_6} - Q'_\chi(\phi) \sin\theta_{E_6}$, where $Q'(\phi, \theta_{E_6})$ is the $U(1)'$ charge resulting from the mixing. A common choice for the angles θ_{E_6} is given in Table 1 for the conventional $U(1)'$ models χ, ψ, η, S, I and N. The superpotential for these models containing Yukawa couplings for quarks and leptons, and including the right-handed neutrino, is:

$$W = Y_u\, \hat{u}\, \hat{q}\, \hat{H}_u - Y_d\, \hat{d}\, \hat{q}\, \hat{H}_d - Y_e\, \hat{e}\, \hat{l}\, \hat{H}_d + \lambda\, \hat{H}_u\, \hat{H}_d\, \hat{S} + Y_\nu\, \hat{l}\, \hat{H}_u\, \hat{\nu}_R \tag{2}$$

where Y_ν is the Yukawa coupling responsible for generating neutrino masses. The $U(1)'$ charge assignments generate the effective μ term, $\mu_{eff} = \lambda\langle S\rangle/\sqrt{2}$. In addition, the Lagrangian contains the soft-breaking terms

$$\begin{aligned}
-\mathcal{L}_{SB,W} &= -A_\lambda S H_d^0 H_u^0 + A_\lambda S H_d^- H_u^+ + A_{d,ij} H_d^0 \tilde{d}^\star_{R,i\alpha} \tilde{d}_{L,i\alpha} + A_{d,ij} H_d^- \tilde{d}^\star_{R,i\alpha} \tilde{u}_{L,i\alpha} \\
&\quad + A_{e,ij} H_d^0 \tilde{e}^\star_{R,i} \tilde{e}_{L,i} - A_{e,ij} H_d^- \tilde{e}^\star_{R,i} \tilde{\nu}_{L,i} - A_{u,ij} H_u^+ \tilde{u}^\star_{R,i\alpha} \tilde{d}_{L,i\alpha} \\
&\quad + A_{u,ij} H_u^0 \tilde{u}^\star_{R,i\alpha} \tilde{u}_{L,i\alpha} + \text{h.c.} \\
-\mathcal{L}_{SB,\Phi} &= m^2_{H_d} |H_d^0|^2 + m^2_{H_d} |H_d^-|^2 + m^2_{H_u} |H_u^0|^2 + m^2_{H_u} |H_u^+|^2 + m^2_S |S|^2 + m^2_{Q,ij} \tilde{d}^\star_{L,i\alpha} \tilde{d}_{L,j\alpha} \\
&\quad + m^2_{d,ij} \tilde{d}^\star_{R,i\alpha} \tilde{d}_{R,j\alpha} + m^2_{L,ij} \tilde{e}^\star_{L,i} \tilde{e}_{L,j} + m^2_{e,ij} \tilde{e}^\star_{L,i} \tilde{e}_{R,j} + m^2_{Q,ij} \tilde{u}^\star_{L,i\alpha} \tilde{u}_{L,j\alpha} \\
&\quad + m^2_{u,ij} \tilde{u}^\star_{R,i\alpha} \tilde{u}_{R,j\alpha} + m^2_{L,ij} \tilde{\nu}^\star_{L,i} \tilde{\nu}_{L,j} + m^2_{\nu,ij} \tilde{\nu}^\star_{R,i} \tilde{\nu}_{R,j} \\
-\mathcal{L}_{SB,\lambda} &= \frac{1}{2} \left(M_1 \lambda^2_{\tilde{B}} + M_2 \lambda^2_{\tilde{W},i} + M_U \lambda^2_{\tilde{Z}'} + M_3 \lambda_{\tilde{g},\alpha} \lambda_{\tilde{g},\beta} + \text{h.c.} \right) .
\end{aligned} \tag{3}$$

3 $U(1)'$ models with universal charges

In the first instance, we assume that the $U(1)'$ charges are generation independent, that is, the Z' gauge bosons couple to the SM matter fields the same way as the Z [12]. The $U(1)'$ charges of the fields must satisfy a number of conditions arising from phenomenological constraints, from gauge invariance, and from the requirement of cancellation of gauge and gravitational anomalies. The disadvantage here is that anomaly cancellation requires introduction of additional exotic matter fields.

$$W_{\text{univ}} \longrightarrow W + \sum_{i=1}^{n_\mathcal{Q}} h_Q^i \widehat{S} \widehat{\mathcal{Q}}_i \widehat{\overline{\mathcal{Q}}}_i + \sum_{j=1}^{n_\mathcal{L}} h_L^j \widehat{S} \widehat{\mathcal{L}}_j \widehat{\overline{\mathcal{L}}}_j \tag{4}$$

Table 2. Gauge quantum numbers of quark $(\widehat{Q}, \widehat{U}, \widehat{D})$, lepton $(\widehat{L}, \widehat{N}, \widehat{E})$, Higgs doublets $(\widehat{H}_u, \widehat{H}_d)$, singlet $\widehat{S}$, exotic quark $(\widehat{\mathcal{Q}}, \widehat{\overline{\mathcal{Q}}})$ and exotic lepton $(\widehat{\mathcal{L}}, \widehat{\overline{\mathcal{L}}})$ superfields.

	$\widehat{Q}$	$\widehat{U}$	$\widehat{D}$	$\widehat{L}$	$\widehat{N}$	$\widehat{E}$	$\widehat{H}_u$	$\widehat{H}_d$	$\widehat{S}$	$\widehat{\mathcal{Q}}$	$\widehat{\overline{\mathcal{Q}}}$	$\widehat{\mathcal{L}}$	$\widehat{\overline{\mathcal{L}}}$
$SU(3)_C$	3	$\overline{3}$	$\overline{3}$	1	1	1	1	1	1	3	$\overline{3}$	1	1
$SU(2)_L$	2	1	1	2	1	1	2	2	1	1	1	1	1
$U(1)_Y$	1/6	−2/3	1/3	−1/2	0	1	1/2	−1/2	0	$Y_{\mathcal{Q}}$	$-Y_{\mathcal{Q}}$	$Y_{\mathcal{L}}$	$-Y_{\mathcal{L}}$
$U(1)'$	Q'_Q	Q'_U	Q'_D	Q'_L	Q'_N	Q'_E	Q'_{H_u}	Q'_{H_d}	Q'_S	$Q'_{\mathcal{Q}}$	$Q'_{\overline{\mathcal{Q}}}$	$Q'_{\mathcal{L}}$	$Q'_{\overline{\mathcal{L}}}$

The anomaly-cancelling conditions are as follows.

The $U(1)'$ charges satisfy $Q'_{H_u} + Q'_{H_d} \neq 0$ to forbid the bare μ term, and $Q'_L + Q'_{H_u} + Q'_N \neq 0$ to induce neutrino masses correctly. Gauge invariance of the superpotential implies

$$\begin{aligned} &0 = Q'_S + Q'_{H_u} + Q'_{H_d}, \qquad 0 = Q'_Q + Q'_{H_u} + Q'_U, \qquad 0 = Q'_Q + Q'_{H_d} + Q'_D, \\ &0 = Q'_L + Q'_{H_d} + Q'_E, \qquad 0 = Q'_{\mathcal{Q}} + Q'_{\overline{\mathcal{Q}}} + Q'_S, \qquad 0 = Q'_{\mathcal{L}} + Q'_{\overline{\mathcal{L}}} + Q'_S. \end{aligned} \tag{5}$$

For the model to be anomaly-free the $U(1)'$ charges of fields must satisfy

$$0 = 3(2Q'_Q + Q'_U + Q'_D) + n_{\mathcal{Q}}(Q'_{\mathcal{Q}} + Q'_{\overline{\mathcal{Q}}}), \tag{6}$$

$$0 = 3(3Q'_Q + Q'_L) + Q'_{H_d} + Q'_{H_u}, \tag{7}$$

$$\begin{aligned} 0 = {} & 3(\frac{1}{6}Q'_Q + \frac{1}{3}Q'_D + \frac{4}{3}Q'_U + \frac{1}{2}Q'_L + Q'_E) + \frac{1}{2}(Q'_{H_d} + Q'_{H_u}) \\ & + 3n_{\mathcal{Q}}Y^2_{\mathcal{Q}}(Q'_{\mathcal{Q}} + Q'_{\overline{\mathcal{Q}}}) + n_{\mathcal{L}}Y^2_{\mathcal{L}}(Q'_{\mathcal{L}} + Q'_{\overline{\mathcal{L}}}), \end{aligned} \tag{8}$$

$$\begin{aligned} 0 = {} & 3(6Q'_Q + 3Q'_U + 3Q'_D + 2Q'_L + Q'_E + Q'_N) + 2Q'_{H_d} + 2Q'_{H_u} \\ & + Q'_S + 3n_{\mathcal{Q}}(Q'_{\mathcal{Q}} + Q'_{\overline{\mathcal{Q}}}) + n_{\mathcal{L}}(Q'_{\mathcal{L}} + Q'_{\overline{\mathcal{L}}}), \end{aligned} \tag{9}$$

$$\begin{aligned} 0 = {} & 3({Q'_Q}^2 + {Q'_D}^2 - 2{Q'_U}^2 - {Q'_L}^2 + {Q'_E}^2) - {Q'_{H_d}}^2 + {Q'_{H_u}}^2 + 3n_{\mathcal{Q}}Y_{\mathcal{Q}}({Q'_{\mathcal{Q}}}^2 - {Q'_{\overline{\mathcal{Q}}}}^2) \\ & + n_{\mathcal{L}}Y_{\mathcal{L}}({Q'_{\mathcal{L}}}^2 - {Q'_{\overline{\mathcal{L}}}}^2), \end{aligned} \tag{10}$$

$$\begin{aligned} 0 = {} & 3(6{Q'_Q}^3 + 3{Q'_D}^3 + 3{Q'_U}^3 + 2{Q'_L}^3 + {Q'_E}^3 + {Q'_N}^3) + 2{Q'_{H_d}}^3 + 2{Q'_{H_u}}^3 + {Q'_S}^3 \\ & + 3n_{\mathcal{Q}}({Q'_{\mathcal{Q}}}^3 + {Q'_{\overline{\mathcal{Q}}}}^3) + n_{\mathcal{L}}({Q'_{\mathcal{L}}}^3 + {Q'_{\overline{\mathcal{L}}}}^3), \end{aligned} \tag{11}$$

which correspond to vanishing of $U(1)'$-$SU(3)_C$-$SU(3)_C$, $U(1)'$-$SU(2)_L$-$SU(2)_L$, $U(1)'$-$U(1)_Y$-$U(1)_Y$, $U(1)'$-graviton-graviton, $U(1)'$-$U(1)'$-$U(1)_Y$, and $U(1)'$-$U(1)'$-$U(1)'$ anomalies, respectively. All these anomaly cancellation conditions are satisfied for a particular pattern of charges and parameters. The solution to the mixed anomaly constraints requires $n_{\mathcal{Q}} = 3$ color triplet pairs with hypercharge $Y_{\mathcal{Q}} = -1/3$, and $n_{\mathcal{L}} = 5$ singlet pairs with hypercharge $Y_{\mathcal{L}} = -\sqrt{2/5}$. The particle content is given in Table 2. For the choices of the $U(1)'$ models in Table 1, these charges can be explicitly parametrized, omitting the exotica, as in Table 3.

After the spontaneous breaking of the symmetry group to electromagnetism, the W, Z and Z' bosons become massive while the photon stays massless. In general there is mixing between the Z and Z' eigenstates, parameterized by a mixing angle $\alpha_{ZZ'}$. However, electroweak precision data strongly constrain $\alpha_{ZZ'}$ to be very small, $\mathcal{O}(10^{-3})$, [15]. At tree level, the squares of the masses of the Z and Z' bosons are

Table 3. $U(1)'$ charges of quark (Q, D, U), lepton (L, E, N) and Higgs (H_u, H_d, S) supermultiplets in anomaly-free $U(1)'$ groups from Table 1.

	$2\sqrt{10}Q'_\chi$	$2\sqrt{6}Q'_\psi$	$2\sqrt{15}Q'_\eta$	$2\sqrt{15}Q'_S$	$2Q'_I$	$2\sqrt{10}Q'_N$
Q, U, E	-1	1	-2	$-1/2$	0	1
L, D	3	1	1	4	-1	2
N	-5	1	-5	-5	1	0
H_u	2	-2	4	1	0	2
H_d	-2	-2	1	$-7/2$	1	-3
S	0	4	-5	5/2	-1	5

given by:

$$m_Z^2 = \frac{g_1^2 + g_2^2}{2}\left(\langle H_u^0\rangle^2 + \langle H_d^0\rangle^2\right), \quad m_{Z'}^2 = g'^2\left(Q_S'^2\langle S\rangle^2 + Q_{H_u}'^2\langle H_u^0\rangle^2 + Q_{H_d}'^2\langle H_d^0\rangle^2\right),$$

with H_d^0 and H_u^0 being the VEVs of the neutral components of the down-type and up-type Higgs fields H_d and H_u and g_1, g_2 and g' being the coupling constants of the $U(1)_Y$, $SU(2)_L$ and $U(1)'$ gauge groups, respectively.

Note that in all the models, the $U(1)'$ charges for leptons are non-zero. However, this changes if $U(1)_Y$ and $U(1)'$ bosons are allowed to mix kinetically [16]. In that case, the gauge Lagrangian becomes

$$\mathcal{L}_{\text{kin}} = -\frac{1}{4}\hat{B}^{\mu\nu}\hat{B}_{\mu\nu} - \frac{1}{4}\hat{Z}'^{\mu\nu}\hat{Z}'_{\mu\nu} - \frac{\sin\chi}{2}\hat{B}^{\mu\nu}\hat{Z}'_{\mu\nu}\,, \tag{12}$$

with $\hat{B}_{\mu\nu}$ and $\hat{Z}'_{\mu\nu}$ the $U(1)_Y$ and $U(1)'$ boson field strength tensors, respectively, and χ the kinetic mixing angle. Diagonalizing the field strengths by a $GL(2,\mathbf{R})$ rotation,

$$\begin{pmatrix}\hat{B}_\mu\\ \hat{Z}'_\mu\end{pmatrix} = \begin{pmatrix}1 & -\tan\chi\\ 0 & \frac{1}{\cos\chi}\end{pmatrix}\begin{pmatrix}B_\mu\\ Z'_\mu\end{pmatrix}, \tag{13}$$

now B_μ and Z'_μ have canonical diagonal kinetic terms. As discussed in references [1, 16], for $m_Z^2 \ll m_{Z'}^2$ and small values of χ, the impact of kinetic mixing on gauge boson masses is negligible, while the impact on the couplings of the Z' boson with fermions is significant, and given by

$$\mathcal{L}_{\text{int}} = -\bar{\psi}_i\gamma^\mu(g_1 Y_i\hat{B}_\mu + g'Q'_i\hat{Z}'_\mu)\psi_i = -\bar{\psi}_i\gamma^\mu(g_1 Y_i B_\mu + g'\bar{Q}_i Z'_\mu)\psi, \tag{14}$$

with $\bar{Q}_i = Q'_i\sec\chi - \frac{g_1}{g'}Y_i\tan\chi$. Leptophobic scenarios can then be obtained requiring $\bar{Q}_L = \bar{Q}_E = 0$ [9–12]. Since $Y_L = -1/2$ and $Y_E = 1$, leptophobia can be achieved only if $Q'_E = -2Q'_L$, requiring $\sin\chi \approx -0.3$. As a result, leptophobic Z' models naturally arise for E_6 mixing angles in the neighbourhood of $\theta_{E_6} \simeq \theta_\eta \pm n\pi$, with n integer, requirement close to the $U(1)'_\eta$ configuration.

With these conditions, we review the constraints on Z' mass in Figure 1. We chose two possibilities for gauge coupling unification: at the M_{GUT} scale (left panel) or at the M_{SUSY} scale (right panel), and compare our predictions with the results from CMS on di-jet searches [17]. One can see that these constraints are much weaker than the di-lepton bounds, and do not impose any restrictions on Z' masses. We then investigate the collider implications for this scenario. We scan over the free parameters, assuming minimal flavor violation, (taking all the flavor-violating parameters of

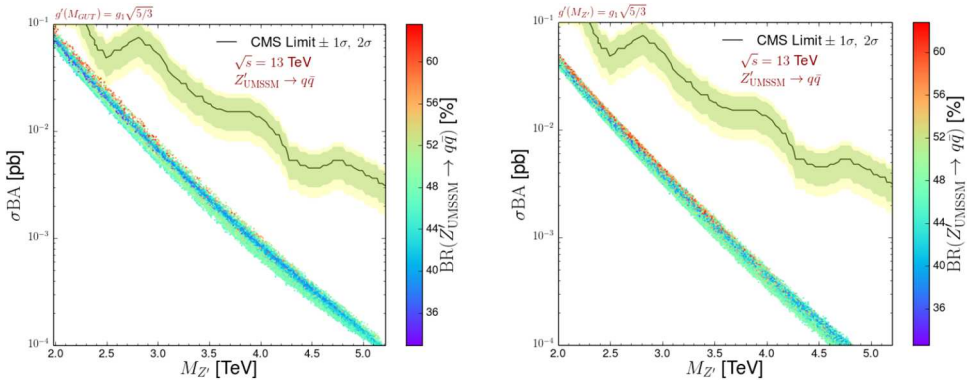

Fig. 1. Z' production cross-section multiplied by the dijet branching ratio and by the acceptance A $\simeq 0.6$, for unification at M_{GUT} scale (left panel) and at M_{SUSY} scale (right panel), comparing NLO QCD theoretical predictions to the bounds obtained by the CMS collaboration [17] at the 1σ (green) and 2σ (yellow) level. The Z' dijet branching ratio is shown for both cases, on the right.

Table 4. Scanning ranges for parameters. For coupling unification at GUT scale, only the four quantities in the top panel are varied.

Parameter	Scanned range	Parameter	Scanned range
m_0	$[0, 3]$ TeV	μ_{eff}	$[-2, 2]$ TeV
$m_{1/2}$	$[0, 5]$ TeV	A_λ	$[-7, 7]$ TeV
A_0	$[-3, 3]$ TeV	$m_{Z'}$	$[1.98, 5.2]$ TeV
$\tan\beta$	$[0, 60]$	θ_{E_6}	$[-\pi, \pi]$
$m^2_{\tilde{q},\tilde{u},\tilde{d}}$	$[0, 16]$ TeV^2	$m_{1,2,3,4}$	$[0, 3]$ TeV
$m^2_{\tilde{e},\tilde{l}}$	$[0, 1]$ TeV^2	$m^2_{\tilde{\nu}}$	$[-6.8, 9]$ TeV^2

the soft supersymmetry-breaking Lagrangian to be vanishing), and enforcing unified boundary conditions on the remaining soft parameters (at GUT or SUSY scales). The parameter ranges are given in Table 4.

To observe light leptophobic Z' bosons, we look for them decaying through a supersymmetric cascade. As direct decays into leptons are forbidden, dilepton final states can nevertheless arise from (Z'-mediated) chargino-pair production followed by decays into charged leptons and missing energy through an intermediate (possibly off-shell) W boson $\tilde{\chi}_1^\pm \to (W^\pm \to l^\pm \nu_l)\ \tilde{\chi}_1^0$, with $\tilde{\chi}_1^0$ being the lightest neutralino. To enhance the signal, we devise benchmarks $U(1)'$ scenarios where the mass difference between the lightest chargino $\tilde{\chi}_1^\pm$ and the lightest neutralino $\tilde{\chi}_1^0$ is at least $m_W \simeq 80$ GeV, not excluded by data, and with different $U(1)'$ properties. The signal process under consideration is

$$pp \to Z' \to \tilde{\chi}_1^+ \tilde{\chi}_1^- \to l^+ l^- + E_{T\text{miss}}\ . \tag{15}$$

Both benchmarks have a Z' boson with a mass of about 2.5 TeV and charginos and neutralinos as light as possible, to maximize the branching ratios in equation (15). **BM I** relies on a $U(1)'_\eta$ symmetry, with $\theta_{E_6} = -0.79\pi$, while the second scenario, **BM II**, is close to $U(1)'_\psi$, with a mixing angle $\theta_{E_6} = 0.2\pi$. The parameters corresponding to these benchmarks are shown in Table 5. For signal analysis, we performed a full Monte Carlo event simulation at the LHC, for $\sqrt{s} = 14$ TeV. The hard-scattering

Table 5. $U(1)'$ parameters for benchmarks **BM I** and **BM II**.

Parameter	θ_{E_6}	$\tan\beta$	$\mu_{\rm eff}$ [GeV]	$M_{Z'}$ [TeV]	M_0 [TeV]	M_1 [GeV]
BM I	$-0.79\ \pi$	9.11	218.9	2.5	2.6	106.5
BM II	$0.2\ \pi$	16.08	345.3	2.5	1.9	186.7
Parameter	M_2 [GeV]	M_3 [TeV]	M_1' [GeV]	A_0 [TeV]	A_λ [TeV]	$\sin\chi$
BM I	230.0	3.6	198.9	2	5.9	-0.35
BM II	545.5	5.5	551.7	1.5	5.1	0.33

Table 6. Cuts employed to enhance signal over background for a leptophobic Z' boson decaying through a supersymmetric cascade. For each cut we list the number of surviving events for an integrated luminosity of 3000 fb^{-1} at $\sqrt{s} = 14$ TeV for background and for signal benchmarks **BM I** and **BM II**, as well as the significances s and Z_A, as defined in equation (17), with 20% uncertainty.

Step	Requirements	Background	**BM I**	**BM II**
0	Initial	1.7×10^{11}	8.8×10^3	1.9×10^4
1	$N^l = 2$	6.1×10^8	401	860
2	Electron veto	2.9×10^8	100	230
3	$\lvert\eta^l\rvert < 1.5$	1.7×10^8	76	170
4	$I^\mu_{\rm rel} < 0.15$	7.9×10^5	63	130
5	$\Delta R(l_1, l_2) > 2.5$	7.9×10^5	62	130
6	Jet veto	7.7×10^4	57	120
7	$p_T(l_1) > 300$ GeV	44	36	71
8	$p_T(l_2) > 200$ GeV	20	19	32
9	$E_{T\rm miss} > 100$ GeV	10	14	27
	s		3.77σ	7.14σ
	Z_A		3.03σ	5.05σ

signal events are generated by MadGraph5_aMC@NLO [18], and we found that the production cross-section is $\sigma(pp \to Z') \simeq 120$ fb for both benchmarks.[1] Parton showers and hadronization were simulated using the Pythia 8.2.19 program [19], and the LHC response was modelled by the Delphes 3.3.2 package [20], using the Snowmass parameterization [21]. We considered an average number of pile-up events of 140 and normalized the results to an integrated integrated luminosity of 3000 fb^{-1}. For the backgrounds, we considered all processes leading to final states with two charged leptons and missing energy, such as vector-boson pairs VV. Since the background is large, cuts were necessary to observe the signal, as shown in Table 6, where we defined two variables, s and Z_A[2] to define the significance of the leptophobic Z'-boson signal,

$$s = \frac{S}{\sqrt{B + \sigma_B^2}}\ , \tag{16}$$

$$Z_A = \sqrt{2\left\{(S+B)\ln\left[\frac{(S+B)(S+\sigma_B^2)}{B^2 + (S+B)\sigma_B^2}\right] - \frac{B^2}{\sigma_B^2}\ln\left[1 + \frac{\sigma_B^2 S}{B(B+\sigma_B^2)}\right]\right\}}\ , \tag{17}$$

with S (B) the number of signal (background) events and σ_B the standard deviation of background events. Our most promising variables are shown in Figure 2. Plots

[1] The cross-section depends on the Z' mass and its coupling constant, which are the same for **BM I** and **BM II**.

[2] This is the Asimov exclusion significance which provides a quantitative measure of the statistical fluctuations in the discovery significance and exclusion limits [22].

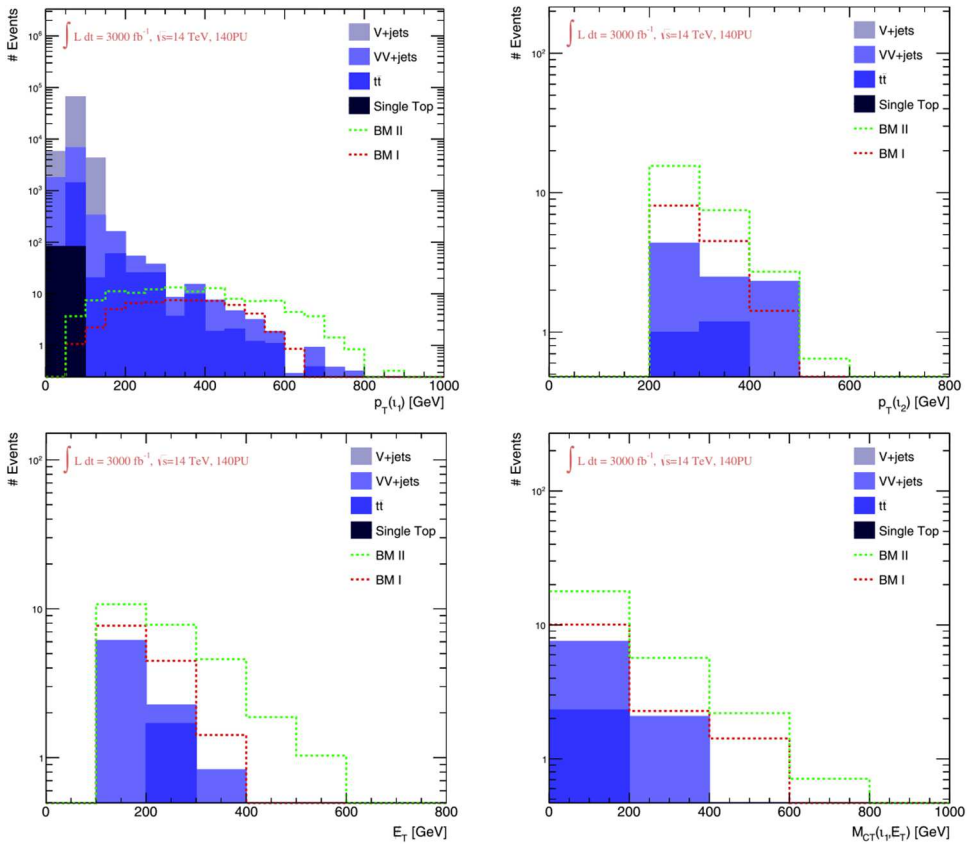

Fig. 2. Top: transverse momentum distribution of the leading muon l_1 (left) and of the next-to-leading muon l_2 (right). Bottom: missing transverse energy spectrum for the background and for the two signal benchmarks (left) and cotransverse mass distributions for muon l_1 and invisible particles leading to missing energy (right). All histograms are obtained after applying all acceptance cuts in Table 6.

given are after applying the first six cuts of Table 6. We give, on top left panel, the distribution in the transverse momentum of the leading muon l_1, while in the top right panel of the figure, we show the transverse-momentum spectrum of the next-to-leading muon l_2. Signal spectra are below the background at low $p_T(l_1)$, while for $p_T(l_1) > 300$ GeV, both signals **BM I** and **BM II** yield comparable numbers of events as the background. The bottom of Figure 2 (left) shows the missing transverse energy due to the lightest neutralinos $\tilde{\chi}_1^0$. The $E_{T\text{miss}}$ are well above the backgrounds, especially above 400 GeV, where the backgrounds are suppressed, while in Figure 2 (bottom right panel), we plot the cotransverse mass M_{CT} for all particles contributing to the missing energy. Thus, for the two benchmark employed, showcasing a light chargino-neutralino spectrum not yet excluded, we obtain visible signals at the LHC, with a significance which varies from 3σ up to even 7σ, according to the criteria employed to estimate the significance.

4 $U(1)'$ models with non-universal charges

Of course, $U(1)'$ models need not arise from breaking of a higher group, but simply as the simplest extension of the SM/MSSM gauge group. We can then explore the

consequences of anomaly-free $U(1)'$ models, without imposing constrains generated by the breaking of $SO(10)$ or E_6. In this case, we also want to construct models where the mass constraints on Z' are relaxed [23]. The advantage here is that anomaly-free $U(1)'$ models *without exotics* exist, but they require allowing flavor non-universality, that is, allowing fermionic family-dependent $U(1)'$ charges [14]. These charges must be chosen so that all anomaly coefficients cancel, including those from mixed anomalies involving $U(1)'$ charges, and gauge-gravity anomalies. These particular theories have received more attention lately, given the LHCb measurements of lepton flavor non-universality in B-meson decays [24,25].

Family dependent $U(1)'$ charge assignments forbid some of the Yukawa couplings in the superpotential, resulting in massless fermions. We must introduce non-holomorphic SUSY breaking Lagrangian terms, induced by the couplings of fermions to the 'wrong' Higgs doublet

$$-\mathcal{L}_c = C_E^{ij} H_u^* \widetilde{L}^i \widetilde{E}_R^{cj} + C_U^{ij} H_d^* \widetilde{Q}^i \widetilde{U}_R^{cj} + C_D^{ij} H_u^* \widetilde{Q}^i \widetilde{D}_R^{cj} + c.c.\,, \tag{18}$$

Fermion masses are now generated at one loop level through sfermion-gaugino loops [14].

For the theory to be anomaly-free, the $U(1)'$ charges must satisfy, as before, conditions requiring vanishing of $U(1)' - SU(3) - SU(3)$, $U(1)' - SU(2) - SU(2)$, $U(1)' - U(1)_Y - U(1)_Y$, $U(1)'$-graviton-graviton, $U(1)' - U(1)' - U(1)_Y$ and $U(1)' - U(1)' - U(1)'$ anomalies. In a family-dependent scenario, the charges for the fields in Table 3 must satisfy, respectively

$$0 = \sum_i (2Q_{Q_i} + Q_{U_i^c} + Q_{D_i})\,, \qquad 0 = \sum_i (3Q_{Q_i} + Q_{L_i}) + Q_{H_d} + Q_{H_u} \tag{19}$$

$$0 = \sum_i (\frac{1}{6}Q_{Q_i} + \frac{1}{3}Q_{D_i^c} + \frac{4}{3}Q_{U_i^c} + \frac{1}{2}Q_{L_i} + Q_{E_i^c}) + \frac{1}{2}(Q_{H_d} + Q_{H_u}) \tag{20}$$

$$0 = \sum_i (6Q_{Q_i} + 3Q_{U_i^c} + 3Q_{D_i^c} + 2Q_{L_i} + Q_{E_i^c}) + 2Q_{H_D} + 2Q_{H_u} + Q_s \tag{21}$$

$$0 = \sum_i (Q_{Q_i}^2 + Q_{D_i^c}^2 - 2Q_{U_i^c}^2 - Q_{L_i}^2 + Q_{E_i^c}^2) - Q_{H_d}^2 + Q_{H_u}^2 \tag{22}$$

$$0 = \sum_i (6Q_{Q_i}^3 + 3Q_{D_i^c}^3 + 3Q_{U_i^c}^3 + 2Q_{L_i}^3 + Q_{E_i^c}^3) + 2Q_{H_d}^3 + 2Q_{H_u}^3 + Q_S^3. \tag{23}$$

There are numerous possibilities for satisfying these relations. These are classified in [26] and various aspects of their phenomenological implications have been studied both within non-SUSY and SUSY frameworks [27–32].

4.1 $U(1)'$ with leptophobic non-universal couplings

We opt here for a simple family dependent choice for supersymmetric $U(1)'$ models with non-universal charges. A possible solution to the above, satisfying the anomaly cancellation requirement is

$$\begin{aligned} &Q_{E_{1,2}^c} = Q_{L_{1,2}} = Q_{L_3} = 0 \\ &Q_{Q_i} = \frac{Q_{E_3^c}}{9}\,;\, Q_{D_i^c} = -\frac{Q_{E_3^c}}{9}\,;\, Q_{U_i^c} = -\frac{Q_{E_3^c}}{9}\,; \\ &Q_{H_u} = 0\,;\, Q_{H_d} = -Q_{E_3^c}\,;\, Q_S = Q_{E_3^c}\,, \end{aligned} \tag{24}$$

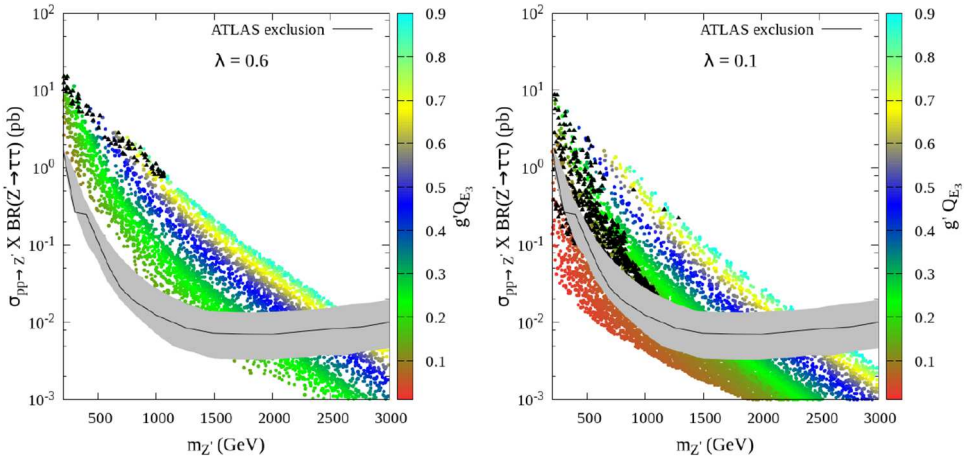

Fig. 3. Effect of the exclusion limits on $m_{Z'}$ from $Z' \to \tau\tau$ search channel for scenarios with $\lambda = 0.6$ (left panel), and $\lambda = 0.1$ (right panel). The color coding represents the LSP neutralino mass or $g' Q_{E_3}$ as indicated in the plots. The black points are ruled out by direct chargino-neutralino searches. The grey shaded region represents the 95% exclusion region around the observed limit.

which is by no means general, but allows us to express all $U(1)'$ charges in terms of a single one, Q_{E_3}. Another possibility is

$$\begin{aligned} &Q_{Q_{1,2}} = Q_{U^c_{1,2}} = Q_{D^c_{1,2}} = Q_{\nu_{R_{1,3}}} = Q_{L_{1,3}} = Q_{E^c_1} = 0 \\ &Q_{U^c_3} = Q_{D^c_3} = Q_{E^c_3} = -\frac{1}{2}\,;\; Q_{E^c_2} = Q_{\nu_{R_2}} = Q_{L_2} = 2; \\ &Q_{H_u} = 0\,;\; Q_{H_d} = \frac{1}{2}\,;\; Q_S = -\frac{1}{2}\,. \end{aligned} \tag{25}$$

We use this charge assignments while performing a scan over the model parameters as follows. Throughout this scan we chose $\lambda = 0.6$ and $\lambda = 0.1$ (thus changing μ_{eff}), $m_1 = m_2 = m_4 = 4$ TeV, and all slepton and squark masses at or above 3 TeV. The exclusion limits, as obtained, are shown in Figure 3, for large $\lambda = 0.6$ on the left side, and low $\lambda = 0.1$, on the right side. The color gradient represents either the variation of the LSP neutralino mass or $g' Q_{E_3}$, as indicated in the right color bars. The exclusion limit obtained from $Z' \to \tau\tau$ search is shown by the black line while the grey shaded area represents the 95% confidence level region around the exclusion line [13]. The black points represent those excluded by direct neutralino-chargino searches [33–35]. For large λ, these constraints do not appear to affect the available parameter space. The higgsino, bino and wino parameters are large throughout, making the chargino states and other neutralino states in the spectrum quite heavy, and the singlino is the LSP state, which can still be significantly light. Thus the NLSP pair or the LSP-NLSP associated production cross-sections are very small. On the other hand, the LSPs can be produced copiously, but they are completely invisible. As expected, the exclusion limit on $m_{Z'}$ becomes weaker as $g' Q_{E_3^c}$ is decreased since the production cross-section drops with it. As evident, with $g' Q_{E_3^c} \sim 0.2$, the exclusion limit can be much weaker, $m_{Z'} \geq 1500$ GeV. For small λ, for small enough $Q_{E_3^c}$, even sub-TeV $m_{Z'}$ is allowed from $Z' \to \tau\tau$ searches. Since the bino and wino soft mass parameters are decoupled from the rest of the spectrum, the LSP can be either a singlino or higgsino. All the allowed points shown in the figure have very small LSP-NLSP mass

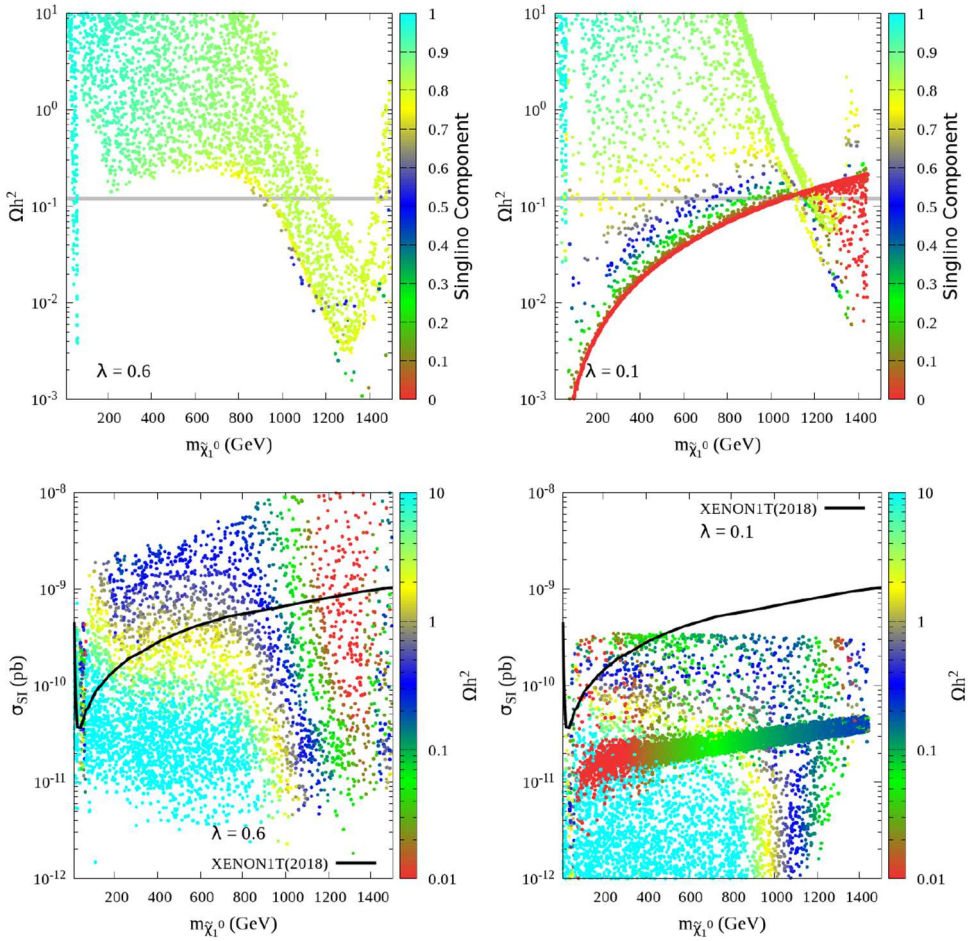

Fig. 4. Distribution of the relic density as a function of the LSP mass with the color gradient representing variation of $m_{Z'}$ (a) and the abundance of the singlino component in the LSP neutralino (b). Plot (c) shows the distribution of direct detection cross-section as a function of LSP mass with the color gradient representing relic density. Left panel and right panel are for $\lambda = 0.6$ and $\lambda = 0.1$, respectively.

gap and hence may avoid detection. We verified that they too are allowed from latest neutralino-chargino search results constraints [33–35].

Now we analyze the DM properties. The distribution of the relic density as a function of the LSP neutralino mass is given in Figure 4 (top) and the spin-independent direct detection cross-section in Figure 4 (bottom). We plot scenarios with $\lambda = 0.6$ (left) and $\lambda = 0.1$ (right).The color coding in the plots indicate (top) the abundance of singlino component in the LSP and (bottom) the relic density. The horizontal shaded band represents the 2σ allowed region around the correct relic abundance, 0.119 ± 0.0054 [36]. The XENON limit [37] on the direct detection cross-section (σ_{SI}) is shown by the black curve. The two distinct resonance regions shown in the figure are due to the two CP-even Higgs masses corresponding to the MSSM Higgs doublets. For small $g'Q_{Ec_3}$ the LSP is dominantly singlino resulting in very small σ_{SI} which increases as the LSP becomes a singlino-higgsino admixture.

Table 7. Basic parameters for the chosen benchmarks **BP1** and **BP2**.

Parameters	Type-I	
& BR	**BP1**	**BP2**
$\tan\beta$	10.0	11.6
Q_{E_3}	0.5	0.5
$g^{'}$	0.3	0.3
λ	0.1	0.1
v_S (GeV)	9203.0	10562.0

From the plots above, we could devise three different classes of benchmark points for the relevant parameter region, depending on whether the LSP is singlino-dominated, higgsino-dominated or a singlino-higgsino admixture, as described above.

- **Type-I:** Masses are aligned in such a way that the Z' can decay into both the higgsino and singlino type neutralino-chargino states. There are three neutralinos and one chargino lighter than $m_{Z'}$ and a sizeable mass gap between LSP singlino and NLSP higgsino states, such that the resulting decayed leptons can be hard enough. This type corresponds to the right panel in Figure 3.
- **Type-II:** The hierarchy of masses are similar as in Type-I, except for the fact that the LSP can be either singlino or higgsino dominated, or a well-mixed state. The NLSP-LSP mass gap is small and the final state leptons are softer. This set of points is also shown in right panel of Figure 3.
- **Type-III:** Only the LSP state is lighter than the Z'. The LSP can either be a singlino or higgsino. The NLSP mass kinematically forbids Z' to decay into any chargino or neutralino pairs, and the Z' has a large invisible branching ratio. This type of points is shown in Figure 3, left panel.

We discuss Type-I and Type-II benchmark points only, since the Z' in Type-III has no visible decay into SUSY particles, and design several representative benchmarks. Among possible choices, we highlight two most promising, **BP1** and **BP2**, both of Type-I (involving hard leptons), summarized in Table 7.

The dominant SM backgrounds for **BP1** and **BP2** are $t\bar{t}+$ jets, $t\bar{t}+V$ ($V = W^{\pm}, Z$), $t\bar{t}+h$, VV, VVV and $Z+$ jets. To distinguish the signal from background, we impose the following cuts:

- **C1:** The final state must have two opposite-sign different-flavor leptons, with transverse momenta, $p_T > 25$ (20) GeV for the leading (sub-leading) leptons.
- **C2:** Allow no central light jets with $p_T > 40$ GeV and $|\eta| < 2.4$.
- **C3:** Allow no central b-tagged jets with $p_T > 20$ GeV and $|\eta| < 2.4$.
- **C4:** The invariant mass of opposite-sign di-leptons pair, $|m_{\ell\ell} - m_Z| > 10$ GeV.
- **C5:** The missing transverse energy, $E_{T\text{miss}} > 200$ GeV.
- **C6:** The stransverse mass, $m_{T_2} = \min_{\boldsymbol{q}_T}[\max(m_T(\boldsymbol{p}_T^{\ell_1}, \boldsymbol{q}_T), m_T(\boldsymbol{p}_T^{\ell_2}, \boldsymbol{p}_T^{\text{miss}} - \boldsymbol{q}_T))] > 150$ GeV, where m_T is given by $m_T(\boldsymbol{p}_T, \boldsymbol{q}_T) = \sqrt{2(p_T q_T - \boldsymbol{p}_T.\boldsymbol{q}_T)}$.

With these, the signal and background are reduced as indicated in Table 8. The reach of HL-LHC would need an integrated luminosity of $\sim$1.4 ab^{-1} and $\sim$2.6 ab^{-1} to exclude (or to achieve 2σ statistical significance) **BP1** and **BP2**, and $\sim$3.1 ab^{-1} and $\sim$6 ab^{-1} integrated luminosity respectively for 3σ significance, most within reach of HL-LHC.

Table 8. Cutflow table for signal and SM background for **BP1** and **BP2** benchmarks.

Channels	Cross-section (fb)					
	C1	**C2**	**C3**	**C4**	**C5**	**C6**
BP1	1.008	0.572	0.544	0.504	0.207	0.007
BP2	0.593	0.330	0.313	0.291	0.133	0.005
$t\bar{t}+$ jets	13823.5	7756.9	423.1	406.6	6.535	–
$t\bar{t}+X$	85.992	37.568	0.546	0.497	0.032	–
VV	1755.233	1362.872	1343.398	1086.805	1.104	0.003
VVV	15.021	4.119	2.966	2.430	0.117	0.012

Table 9. Quantum numbers for the anomaly-free $U(1)'$ gauge group in the model.

$Q_{1,2}$	0	L_1,E_1^c	0	S	$-1/2$
Q_3	$+1/2$	L_2	-2	ν_2^c	$+2$
$U_{1,2}^c$,$D_{1,2}^c$	0	L_3	0	ν_1^c, ν_3^c	0
U_3^c	-1/2	E_2^c	$+2$	H_u	0
D_3^c	$-1/2$	E_3^c	-1/2	H_d	$+1/2$

4.2 $U(1)'$ with quarkophobic non-universal couplings

To circumvent mass limits on the Z' gauge boson, we could choose an anomaly-free $U(1)'$ symmetry coupling non-universally to the quark sector. In particular, if only the third generation quarks are charged under this $U(1)'$, this scenario can easily evade the dilepton bound from the LHC searches. The allowed parameter space this $U(1)'$ model can accommodate the R_K and R_{K^*} anomalies in B-physics [24,25] and considerably weaken the Z' mass limits while remaining perturbative up to the Planck scale [38]. In Table 9 we list a choice of such $U(1)'$ charges, satisfying equations (19)–(23), where only the third family of quarks carries non-zero hypercharge. In this scenario Z' does not couple to the first two generations of quarks, rendering its production cross-section very small, and thus evading the mass constraints from the LHC. We show that this can also explain the anomalies in B-physics. The effective Lagrangian responsible for the B meson decay is given by the contribution of $\mathcal{O}_9$ operator, integrating out the Z' (note that $\mathcal{O}_{10}$ does not contribute, due to the vector-like coupling of the Z'):

$$\mathcal{L}_{\mathcal{O}_9} = -\frac{c_{\theta_q} s_{\theta_q}}{m_{Z'}^2} g'^2 \bar{s}_L \gamma^\mu b_L \bar{\mu} \gamma_\mu \mu,$$

$$\text{yielding} \quad C_9^\mu = -\frac{\pi}{\alpha \sqrt{2} G_F V_{tb} V_{ts}^*} \frac{2 c_{\theta_q} s_{\theta_q}}{m_{Z'}^2} g'^2 \,. \tag{26}$$

The allowed range of the Wilson coefficient is $C_9^\mu \in [-2.12, -1.1]([-2.87, -0.7])$ at $1(2)\ \sigma$ level [39]. The explanation of B decay anomalies requires the couplings of b_L and s_L corresponding to the $U(1)'$ to be non-zero. This is achieved through rotating the flavor eigenstates to the mass eigenstates, without triggering large mixing in right-handed down quark sector, by means of a non-zero m_d^{23} element in the down type quarks mass matrix. This mass term can arise from the superpotential $W \supset Y_d^{23} Q_2 H_d D_3^c$, yielding a mixing angle θ_q between b_L and s_L. The global fit to $B_s - \bar{B}_s$ mass mixing, and the CKM fit give an upper bound $|g'^2 c_{\theta_q}^2 s_{\theta_q}^2 / 8 m_{Z'}^2| < 1/(210\,\text{TeV})^2$ [40]. Figure 5, left panel, shows that the $B_s - \bar{B}_s$ mixing measurement requires the mixing angle $|\theta_q| < 0.3$ for $m'_Z/g' = 20$ TeV, while the constraints from $D^0 - \bar{D}^0$

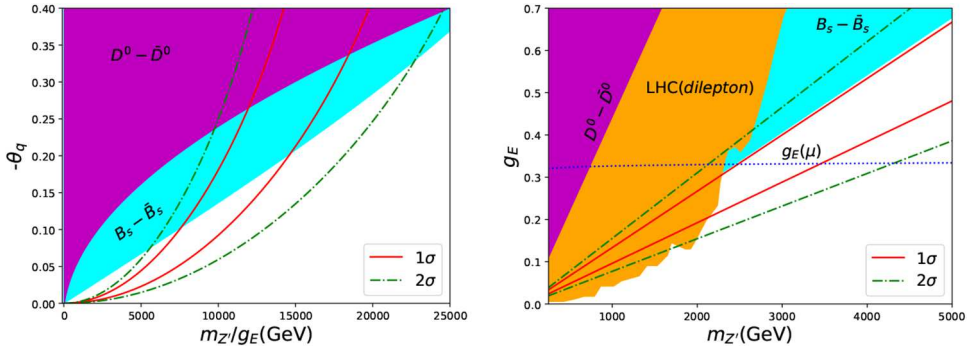

Fig. 5. Fits to the $B_s - \bar{B}_s$, $D^0 - \bar{D}^0$, restricted by the $s_L - b_L$ mixing angle θ_q, coupling $g' =\equiv g_E$, and $m_{Z'}$. Regions between the two solid (dashed) curves are consistent with R_K, R_{K^*} anomaly at $1(2)\sigma$ level, while the shaded regions are excluded by neutral meson mixing and the LHC dilepton searches [41]. The region above the dotted horizontal curve in the right panel is excluded by the Landau pole requirement.

mixing require $|g'^2 c_D^2/8m_{Z'}^2| < 1/(1900\,\text{TeV})^2$ [40] and thus weaker than the $B_s - \bar{B}_s$ mixing, due to the additional CKM suppression of c_D.

While the Z' production rate is suppressed by parton distribution functions of the b quark at the LHC, the branching ratio $BR(Z' \to \mu^+\mu^-)$ is large, so that $\sigma(pp \to Z') \times BR(Z' \to \mu^+\mu^-)$ is sizeable. From Figure 5 (right panel), the LHC dilepton searches can cover $m_{Z'} < 2.5$ TeV for $g' \sim 0.3$, a sizeable reduction in the expected mass of the $m_{Z'}$ from the ATLAS expectation [41], where $m_{Z'} \sim 4.1$ TeV.

5 Conclusion

Motivated by the latest ATLAS and CMS measurements which imposed restrictive lower bounds on the Z' mass, we analyzed models with an additional $U(1)'$ gauge symmetry group where these limits can be relaxed. First, in models arising from the breaking of E_6 supersymmetric GUT, we explored loopholes in the searches carried out at the LHC, by allowing Z' to be leptophobic. We analyzed the Z' decay into supersymmetric final states, such as chargino pairs and showed that supersymmetric decays of leptophobic Z' bosons are capable of giving detectable di-lepton signals, which can be easily discriminated from the backgrounds and from non-supersymmetric Z' events, so far employed to set the exclusion limits.

Extending MSSM by an additional $U(1)'$ gauge group, and allowing the charges for fermions and Higgs bosons to be family dependent, anomalies are cancelled without the introduction of exotica. The disadvantage here is the presence of non-holomorphic terms, giving fermion masses at loop-level. In one possible solution, all the $U(1)'$ charges are written in terms of a single one, Q_{E_3}. The Z' cannot decay into electron or muon pairs at the tree level. The restriction on $m_{Z'}$ arises from Z' decay into $\tau\bar{\tau}$, which is considerably weaker. While the signal cross-section is dependent on the choice of $U(1)'$ charges and other possible decay modes of Z', we showed that the decay into multiple chargino and neutralino states gives rise to observable leptonic signals at the HL-LHC. Non-standard neutralino DM candidates such as a singlino or a higgsino arise naturally for a light Z'. The study of possible signal regions revealed that the di-tau final state is likely to be observed first and that one can use the leptonic signal regions as confirmirmation channels.

When the Z' couples to third generation quarks only, its production cross-section is significantly suppressed even though $BR(Z' \to \mu^+\mu^-)$ is significant. In this scenario, the R_K and R_{K^*} anomalies from B decays have a solution, while at the same time, the $m_{Z'}$ mass bound is significantly relaxed.

In addition, in the present framework, any observation of such leptonic signals at high integrated luminosity will also indicate the presence of SUSY.

The work described in this review was performed in [12,23,38], from where the numerical and graphical analysis are reproduced. I thank Jack Araz, Gennaro Corcella, Guang Hua Duan, Xiang Fan, Benjamin Fuks, Chengcheng Han, Katri Huitu, Subhadeep Mondal and Jin Min Yang for discussions and collaborations. This work was supported in part by NSERC of Canada under grant number SAP105354.

Author contribution statement

The work described in this paper is based on references [12,23,38]. Most of the numerical work was performed by Jack Araz, Subhadeep Mondal and Guang Hua Duan, while the rest of the authors contributed equally in choosing the topic, planning the extent of the work, testing the results, suggesting new directions and refinements of the analysis, as well as comparison with experimental results. All authors contributed to drafting the manuscripts.

References

1. P. Langacker, Rev. Mod. Phys. **81**, 1199 (2009)
2. J.L. Hewett, T.G. Rizzo, Phys. Rep. **183**, 193 (1989)
3. M. Cvetic, D.A. Demir, J.R. Espinosa, L.L. Everett, P. Langacker, Phys. Rev. D **56**, 2861 (1997) [Erratum: Phys. Rev. D **58**, 119905 (1998)]
4. G. Aad et al. [ATLAS Collaboration], Phys. Lett. B **796**, 68 (2019)
5. M. Aaboud et al. [ATLAS Collaboration], Phys. Rev. D **99**, 092004 (2019)
6. A.M. Sirunyan et al. [CMS Collaboration], JHEP **1808**, 130 (2018)
7. G. Arcadi, M.D. Campos, M. Lindner, A. Masiero, F.S. Queiroz, Phys. Rev. D **97**, 043009 (2018)
8. D. Hooper, Phys. Rev. D **91**, 035025 (2015)
9. K.S. Babu, C.F. Kolda, J. March-Russell, Phys. Rev. D **54**, 4635 (1996)
10. D. Suematsu, Phys. Rev. D **59**, 055017 (1999)
11. C.W. Chiang, T. Nomura, K. Yagyu, JHEP **1405**, 106 (2014)
12. J.Y. Araz, G. Corcella, M. Frank, B. Fuks, JHEP **1802**, 092 (2018)
13. M. Aaboud et al. [ATLAS Collaboration], JHEP **1801**, 055 (2018)
14. D.A. Demir, G.L. Kane, T.T. Wang, Phys. Rev. D **72**, 015012 (2005)
15. J. Erler, P. Langacker, T.J. Li, Phys. Rev. D **66**, 015002 (2002)
16. K.S. Babu, C.F. Kolda, J. March-Russell, Phys. Rev. D **57**, 6788 (1998)
17. A.M. Sirunyan et al. [CMS Collaboration], Phys. Lett. B **769**, 520 (2017) [Erratum: Phys. Lett. B **772**, 882 (2017)]
18. J. Alwall et al., JHEP **1407**, 079 (2014)
19. T. Sjostrand et al., Comput. Phys. Commun. **191**, 159 (2015)
20. J. de Favereau et al. [DELPHES 3 Collaboration], JHEP **1402**, 057 (2014)
21. J. Anderson et al., arXiv:1309.1057 [hep-ex]
22. G. Cowan, K. Cranmer, E. Gross, O. Vitells, Eur. Phys. J. C **71**, 1554 (2011)

23. M. Frank, K. Huitu, S. Mondal, Phys. Rev. D **100**, 11, 115018 (2019)
24. R. Aaij et al. [LHCb Collaboration], Phys. Rev. Lett. **113**, 151601 (2014)
25. R. Aaij et al. [LHCb Collaboration], JHEP **1708**, 055 (2017)
26. B.C. Allanach, J. Davighi, S. Melville, JHEP **1902**, 082 (2019) [Erratum: JHEP **1908**, 064 (2019)]
27. A. Celis, J. Fuentes-Martin, M. Jung, H. Serodio, Phys. Rev. D **92**, 015007 (2015)
28. B.C. Allanach, J.M. Butterworth, T. Corbett, JHEP **1908**, 106 (2019)
29. S.F. Mantilla, R. Martinez, F. Ochoa, Phys. Rev. D **95**, 095037 (2017)
30. Y. Tang, Y.L. Wu, Chin. Phys. C **42**, 033104 (2018)
31. J.F. Kamenik, Y. Soreq, J. Zupan, Phys. Rev. D **97**, 035002 (2018)
32. B. Coleppa, S. Kumar, A. Sarkar, Phys. Rev. D **98**, 095009 (2018)
33. G. Aad et al. [ATLAS Collaboration], JHEP **1405**, 071 (2014)
34. M. Aaboud et al. [ATLAS Collaboration], Phys. Rev. D **97**, 052010 (2018)
35. M. Aaboud et al. [ATLAS Collaboration], Phys. Rev. D **98**, 092012 (2018)
36. G. Hinshaw et al. [WMAP Collaboration], Astrophys. J. Suppl. **208**, 19 (2013)
37. E. Aprile et al. [XENON Collaboration], Phys. Rev. Lett. **121**, 111302 (2018)
38. G.H. Duan, X. Fan, M. Frank, C. Han, J.M. Yang, Phys. Lett. B **789**, 54 (2019)
39. W. Altmannshofer, P. Stangl, D.M. Straub, Phys. Rev. D **96**, 055008 (2017)
40. P. Arnan, L. Hofer, F. Mescia, A. Crivellin, JHEP **1704**, 043 (2017)
41. M. Aaboud et al. [ATLAS Collaboration], JHEP **1710**, 182 (2017)